

# Analysis of $D_s DK^*$ and $D_s D^* K^*$ vertices and branching ratio of $B^+ \rightarrow K^{*0} \pi^+$

M. Janbazi<sup>1,a</sup>, R. Khosravi<sup>2,b</sup>

<sup>1</sup> Young Researchers and Elites Club, Shiraz Branch, Islamic Azad University, Shiraz, Iran

<sup>2</sup> Department of Physics, Isfahan University of Technology, Esfahān 84156-83111, Iran

Received: 4 January 2018 / Accepted: 13 July 2018 / Published online: 28 July 2018

© The Author(s) 2018

**Abstract** In this paper, the strong form factors and coupling constants of  $D_s DK^*$  and  $D_s D^* K^*$  vertices are investigated within the three-point QCD sum rules method with and without the  $SU_f(3)$  symmetry. In this calculation, the contributions of the quark–quark, quark–gluon, and gluon–gluon condensate corrections are considered. As an example of specific application of these coupling constants, the branching ratio of the hadronic decay  $B^+ \rightarrow K^{*0} \pi^+$  is analyzed based on the one-particle-exchange which is one of the phenomenological models. In this model,  $B$  decays into a  $D_s D^*$  intermediate state, and then these two particles exchange a  $D(D^*)$  producing the final  $K^*$  and  $\pi$  mesons. In order to compute the effect of these interactions, the  $D_s DK^*$  and  $D_s D^* K^*$  form factors are needed.

## 1 Introduction

In high energy physics, investigation of meson interactions depends on information about the proper functional form of strong form factors. Among all vertices, the charmed meson ones, which play an important role in understanding the final-state re-scattering effects in the hadronic  $B$  decays, are much more significant. They are related to the basic parameters  $\beta$  and  $\lambda$  in the heavy quark effective Lagrangian [1]. Therefore, researchers have concentrated on computing the strong form factors and coupling constants connected to these vertices. Until now, the vertices involving charmed mesons such as  $D^* D^* \rho$  [2],  $D^* D \pi$  [3,4],  $DD\rho$  [5],  $D^* D \rho$  [6],  $DDJ/\psi$  [7],  $D^* DJ/\psi$  [8],  $D^* D_s K$ ,  $D_s^* DK$ ,  $D_0^* D_s K$ ,  $D_{s0}^* DK$  [9],  $D^* D^* P$ ,  $D^* DV$ ,  $DDV$  [10],  $D^* D^* \pi$  [11],  $D_s D^* K$ ,  $D_s^* DK$  [12],  $DD\omega$  [13],  $D_s D_s V$ ,  $D_s^* D_s^* V$  [14,15], and  $D_1 D^* \pi$ ,  $D_1 D_0 \pi$ ,  $D_1 D_1 \pi$  [16] have been studied within the framework of the QCD sum rules.

<sup>a</sup> e-mail: mehdijanbazi@yahoo.com

<sup>b</sup> e-mail: rezakhosravi@cc.iut.ac.ir

The effective Lagrangians for the interaction  $D_s DK^*$  and  $D_s D^* K^*$  vertices are as follows: [17]:

$$\begin{aligned} \mathcal{L}_{D_s DK^*} &= ig_{D_s DK^*} K^{*\alpha} (\bar{D}_s \partial_\alpha D - \partial_\alpha \bar{D}_s D), \\ \mathcal{L}_{D_s D^* K^*} &= -g_{D_s D^* K^*} \epsilon^{\alpha\beta\rho\sigma} \partial_\alpha D_\beta^* (\partial_\rho K_\sigma^* \bar{D}_s \\ &\quad + D_s \partial_\rho \bar{K}_\sigma^*), \end{aligned} \quad (1)$$

where  $g_{D_s DK^*}$  and  $g_{D_s D^* K^*}$  are the strong form factors. From these Lagrangians, the elements related to the  $D_s DK^*$  and  $D_s D^* K^*$  vertices can be derived in terms of the strong form factors as:

$$\begin{aligned} \langle D(p) K^*(q, \varepsilon^K) | D_s(p') \rangle &= -g_{D_s DK^*}(q^2) \times (p^\mu + p'^\mu) \varepsilon_\mu^K(q), \\ \langle D^*(p, \varepsilon^D) K^*(q, \varepsilon^K) | D_s(p') \rangle &= ig_{D_s D^* K^*}(q^2) \times \epsilon^{\alpha\beta\mu\nu} p'_\alpha q_\beta \varepsilon_\mu^D(p) \varepsilon_\nu^K(q), \end{aligned} \quad (2)$$

where  $q = p - p'$ .

In this work, we decide to calculate the strong form factors and coupling constants associated with the  $D_s DK^*$  and  $D_s D^* K^*$  vertices in the frame work of the three-point QCD sum rules (3PSR). As an example of specific application of these coupling constants can be pointed out to branching ratio calculations of hadronic  $B$  decays. In this paper, we would like to consider the branching ratio of the  $B^+ \rightarrow K^{*0} \pi^+$  decay according to the coupling constants of the  $D_s DK^*$  and  $D_s D^* K^*$  vertices.

The plan of the present paper is as follows: In Sect. 2, the strong form factor calculation of the  $D_s DK^*$  vertex is derived in the framework of the 3PSR; computing the quark–quark, quark–gluon and gluon–gluon condensate contributions in the Borel transform scheme. Using necessary changes in the expression obtained for the  $g_{D_s DK^*}$ , the strong form factor  $g_{D_s D^* K^*}$  is presented. In Sect. 3, we analyze the strong form factors as well as the coupling constants with and without the  $SU_f(3)$  symmetry. For a better analysis, a comparison is made between our results and the predictions

of other methods. Finally, we consider the branching ratio of the  $B^+ \rightarrow K^{*0}\pi^+$  decay using the coupling constants of the  $D_s DK^*$  and  $D_s D^* K^*$  vertices.

### 2 Strong form factors of $D_s DK^*$ and $D_s D^* K^*$ vertices

To compute the strong form factors of the  $D_s DK^*$  and  $D_s D^* K^*$  vertices via the 3PSR, we start with the following correlation functions as

$$\begin{aligned} \Pi_\mu^{K^*}(p, p') &= i^2 \int d^4x d^4y \\ &\times e^{ip'x} e^{-i(p'-p)y} \left\langle 0 \left| \mathcal{T} \left\{ j^{D_s}(x) j_\mu^{K^{*\dagger}}(y) j^{D^\dagger}(0) \right\} \right| 0 \right\rangle, \\ \Pi_{\mu\nu}^{K^*}(p, p') &= i^2 \int d^4x d^4y \\ &\times e^{ip'x} e^{-i(p'-p)y} \left\langle 0 \left| \mathcal{T} \left\{ j^{D_s}(x) j_\mu^{K^{*\dagger}}(y) j_\nu^{D^{*\dagger}}(0) \right\} \right| 0 \right\rangle, \end{aligned} \tag{3}$$

$$\begin{aligned} \Pi_\mu^{K^*} &= - \frac{\langle 0 | j^{D_s} | D_s(p') \rangle \langle D_s(p') | K^*(q, \varepsilon^K) D(p) \rangle \langle K^*(q, \varepsilon^K) | j_\mu^{K^{*\dagger}} | 0 \rangle \langle D(p) | j^{D^\dagger} | 0 \rangle}{(p^2 - m_D^2)(p'^2 - m_{D_s}^2)(q^2 - m_{K^*}^2)} + \text{higher and continuum states}, \\ \Pi_\mu^D &= - \frac{\langle 0 | j^{D_s} | D_s(p') \rangle \langle D_s(p') | D(q) K^*(p, \varepsilon^K) \rangle \langle D(q) | j^{D^\dagger} | 0 \rangle \langle K^*(p, \varepsilon^K) | j_\mu^{K^{*\dagger}} | 0 \rangle}{(p^2 - m_{K^*}^2)(p'^2 - m_{D_s}^2)(q^2 - m_D^2)} + \text{higher and continuum states}. \end{aligned} \tag{5}$$

where  $K^*$  is supposed as an off-shell meson. For off-shell charmed mesons, the correlation functions are:

$$\begin{aligned} \Pi_\mu^D(p, p') &= i^2 \int d^4x d^4y \\ &\times e^{ip'x} e^{-i(p'-p)y} \left\langle 0 \left| \mathcal{T} \left\{ j^{D_s}(x) j^{D^\dagger}(y) j_\mu^{K^{*\dagger}}(0) \right\} \right| 0 \right\rangle, \\ \Pi_{\mu\nu}^{D^*}(p, p') &= i^2 \int d^4x d^4y \\ &\times e^{ip'x} e^{-i(p'-p)y} \left\langle 0 \left| \mathcal{T} \left\{ j^{D_s}(x) j_\nu^{D^{*\dagger}}(y) j_\mu^{K^{*\dagger}}(0) \right\} \right| 0 \right\rangle, \end{aligned} \tag{4}$$

where  $j^{D_s} = \bar{c}\gamma_5 s$ ,  $j^D = \bar{c}\gamma_5 u$ ,  $j^{D^*} = \bar{c}\gamma_\mu u$ , and  $j_\mu^{K^*} = \bar{u}\gamma_\mu s$  are interpolating currents with the same quantum numbers of  $D_s$ ,  $D$ ,  $D^*$ , and  $K^*$  mesons, respectively. Also,  $\mathcal{T}$  is time ordering product,  $p$  and  $p'$  are the four momentum of the initial and final mesons, respectively, as depicted in Fig. 1.

To calculate the strong form factor of the  $D_s DK^*$  vertex in the framework of the 3PSR, the correlation functions in Eqs. (3) and (4) are calculated in two different ways. First, they are calculated in the space-like region in terms of quark-gluon language like quark-quark, gluon-gluon condensate, etc. using the Wilson operator product expansion (OPE). It is called the QCD or theoretical side of the QCD sum rules.

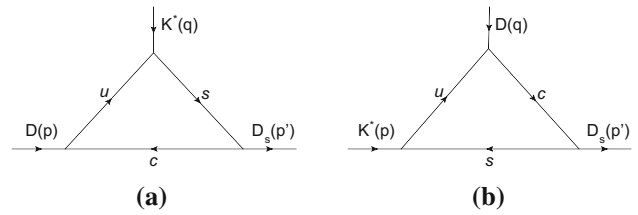


**Fig. 1** Perturbative diagrams for off-shell  $K^*$  (a) and off-shell  $D$  meson (b)

Second, in the hadronic representation, they are calculated in the time-like region in terms of hadronic parameters such as the form factors, decay constants and masses. It is named the phenomenological or physical side.

In order to calculate the phenomenological part of the correlation functions in Eqs. (3) and (4), three complete sets of intermediate states with the same quantum number should be inserted in these equations. Performing the Fourier transformation, for the phenomenological parts, we have:

The matrix elements  $\langle 0 | j_\mu^{K^*} | K^*(q, \varepsilon^K) \rangle$ , and  $\langle 0 | j^{D(s)} | D(s)(p) \rangle$  are defined as:

$$\begin{aligned} \langle 0 | j_\mu^{K^*} | K^*(q, \varepsilon^K) \rangle &= m_{K^*} f_{K^*} \varepsilon_\mu^K(q), \\ \langle 0 | j^{D(s)} | D(s)(p) \rangle &= \frac{m_{D(s)}^2 f_{D(s)}}{m_c + m_{u(s)}}, \end{aligned} \tag{6}$$

where  $m_{K^*}$ ,  $m_{D(s)}$ ,  $f_{K^*}$ , and  $f_{D(s)}$  are the masses and decay constants of mesons  $K^*$  and  $D(s)$ , respectively.  $\varepsilon_\mu$  is the polarization vector of the vector meson  $K^*$ .

We should choose one of the Lorentz structures appearing in Eq. (2) and compute  $\Pi_\mu^{K^*}$  and  $\Pi_\mu^D$  in terms of the strong form factors. As can be seen in Eq. (2), the form factor  $g_{D_s DK^*}$  is the same for two the Lorentz structures  $p_\mu$  and  $p'_\mu$ , and thus can be extracted from sum rules for each of them. But we must choose the Lorentz structure which has fewer ambiguities in the 3PSR approach, which means, less influence of the condensates of higher dimension, and a better stability as a function of the Borel mass parameter [3]. With these conditions, we choose the  $p_\mu$  structure. However, our calculations show that the results for the  $p'_\mu$  structure is exactly the same as this for  $p_\mu$ . Therefore in this case, we could work with any of the structures appearing in Eq. (2).

Inserting Eqs. (2) and (6) in Eq. (5) and after some calculations, we obtain  $\Pi_\mu^{K^*}$  and  $\Pi_\mu^D$  in terms of the strong form factors  $g_{D_s DK^*}^{K^*}$  and  $g_{D_s DK^*}^D$  as:

$$\begin{aligned} \Pi_\mu^{K^*} &= -g_{D_s D K^*}^{K^*}(q^2) \\ &\times \frac{m_{K^*} m_D^2 m_{D_s}^2 f_{K^*} f_D f_{D_s}}{m_c(m_c + m_s)(p^2 - m_D^2)(p^2 - m_{D_s}^2)(q^2 - m_{K^*}^2)} P_\mu \\ &+ \text{higher and continuum states,} \\ \Pi_\mu^D &= -g_{D_s D K^*}^D(q^2) \\ &\times \frac{m_{D_s}^2 m_D^2 f_{K^*} f_D f_{D_s} (q^2 - m_D^2 - m_{K^*}^2)}{2 m_c(m_c + m_s) m_{K^*} (p^2 - m_{K^*}^2)(p^2 - m_{D_s}^2)(q^2 - m_D^2)} P_\mu \\ &+ \text{higher and continuum states.} \end{aligned} \tag{7}$$

In the theoretical side, the three-point correlation function contains the perturbative and non-perturbative parts as

$$\Pi_\mu^{K^*(D)} = (\Pi_{per}^{K^*(D)} + \Pi_{nonper}^{K^*(D)}) P_\mu + \text{other structures.} \tag{8}$$

According to the 3PSR method, we can estimate the perturbative part of the correlation function, using the double dispersion relation, as

$$\begin{aligned} \Pi_{per}^{K^*(D)} &= -\frac{1}{4\pi^2} \int ds \int ds' \frac{\rho^{K^*(D)}}{(s - p^2)(s' - p'^2)} \\ &+ \text{subtraction terms,} \end{aligned} \tag{9}$$

where  $\rho^{K^*(D)}$  is spectral density. The spectral density is calculated in terms of the usual Feynman integrals by the help of the Cutkosky rules, where the quark propagators are replaced by Dirac-delta functions, i.e.,  $\frac{1}{p^2 - m^2} \rightarrow (-2\pi i)\delta(p^2 - m^2)$ . The diagrams corresponding to the perturbative part (bare loop) are depicted in Fig. 1. Using Fig. 1 and after some straightforward calculations, we have:

- For the off-shell  $K^*$  (Fig. 1a):

$$\begin{aligned} \rho_{D_s D K^*}^{K^*} &= 6I_0[2m_c m_s - 2m_c^2 \\ &+ \Delta' + C_1'(2m_c m_s - 2m_c^2 + u)]. \end{aligned}$$

- For the off-shell  $D$  (Fig. 1b):

$$\begin{aligned} \rho_{D_s D K^*}^D &= 6I_0[2m_c m_s - 2m_s^2 + \Delta \\ &+ C_1(2m_c m_s - 2m_s^2 + 2\Delta + u)]. \end{aligned}$$

The explicit expressions of the coefficients in the spectral densities are given in Appendix A.

Now, the non-perturbative part contributions to the correlation function are discussed. In QCD, the correlation function can be evaluated by OPE in the deep Euclidean region. Using the expansion of it in terms of a series of local operators with increasing dimension, we get:

$$\begin{aligned} \Pi_\mu &= C_\mu^{(0)} I + C_\mu^{(3)} \langle 0 | \bar{\Psi} \Psi | 0 \rangle \\ &+ C_\mu^{(4)} \langle 0 | G_{\rho\nu}^a G_a^{\rho\nu} | 0 \rangle + C_\mu^{(5)} \langle 0 | \bar{\Psi} \sigma_{\rho\nu} T^a G_a^{\rho\nu} \Psi | 0 \rangle \\ &+ C_\mu^{(6)} \langle 0 | \bar{\Psi} \Gamma \Psi \bar{\Psi} \Gamma' \Psi | 0 \rangle + \dots, \end{aligned} \tag{10}$$

where  $C_\mu^{(i)}$  are the Wilson coefficients,  $I$  is the unit operator,  $\bar{\Psi}$  is the local fermion field operator and  $G^{\rho\nu}$  is the gluon strength tensor. The Wilson coefficient  $C_\mu^{(0)}$  is the contribution of the perturbative part of QCD (i.e.,  $\Pi_{per}^{K^*(D)}$ ), and the

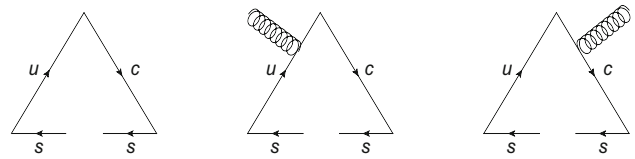


Fig. 2 Non-perturbative diagrams for the off-shell  $D$  meson

other coefficients are contributions of the non-perturbative part ( $\Pi_{nonper}^{K^*(D)}$ ). It is important to note that in above equation,  $C_\mu^{(5)} \langle 0 | \bar{\Psi} \sigma_{\rho\nu} T^a G_a^{\rho\nu} \Psi | 0 \rangle \equiv m_0^2 C_\mu^{(5)} \langle 0 | \bar{\Psi} \Psi | 0 \rangle$  [18]. Therefore, we can collect the coefficients  $C_\mu^{(3)}$  and  $C_\mu^{(5)}$  as  $(C_\mu^{(3)} + m_0^2 C_\mu^{(5)}) \langle 0 | \bar{\Psi} \Psi | 0 \rangle$ , where  $m_0^2 = 0.8 \pm 0.2 \text{ GeV}^2$  [18].

In Eq. (10), the Wilson coefficients  $C_\mu^{(3)}$ ,  $C_\mu^{(4)}$  and  $C_\mu^{(5)}$  of dimensions 3, 4 and 5 are related to contributions of the quark–quark, gluon–gluon and quark–gluon condensate, respectively. Also,  $C_\mu^{(6)}$  is connected to contribution of the four-quark condensate of dimension six. For the calculation of the condensate terms, we consider these points:

- Our calculations show that the contributions of the four-quark condensate are less than a few percent, therefore the condensate terms of dimensions 3, 4 and 5 are more important than the other terms in OPE.
- In the 3PSR, when the light quark is a spectator, the gluon–gluon condensate contributions can be easily ignored [18].
- The quark condensate contribution of the light quark which is a non spectator, is zero after applying the double Borel transformation with respect to the both variables  $p^2$  and  $p'^2$ , because only one variable appears in the denominator.
- In the 3PSR, when the heavy quark is a spectator, the quark–quark condensate contributions are suppressed by inverse of the heavy quark mass, and can be safely omitted [18].

Therefore, to compute the contribution of the non-perturbative part of the correlation function for the off-shell  $D$  meson, three diagrams of dimensions 3 and 5, shown in Fig. 2, are considered. In this case, the quark–quark and quark–gluon diagrams are more important than the other terms in the OPE since the light quark  $s$  is a spectator.

For a better analysis, we compare the contributions of the quark–quark plus quark–gluon condensates with the gluon–gluon condensate for the off-shell  $D$  meson, by applying the Borel transformation, in the interval  $5 \text{ GeV}^2 \leq Q^2 \leq 16 \text{ GeV}^2$  ( $Q^4 = -q^2$ ) in Fig. 3. As can be seen, the gluon–gluon condensate contributions can be easily ignored.

When  $K^*$  is an off-shell meson, the gluon–gluon diagrams of dimension 4 are more important than the quark–quark

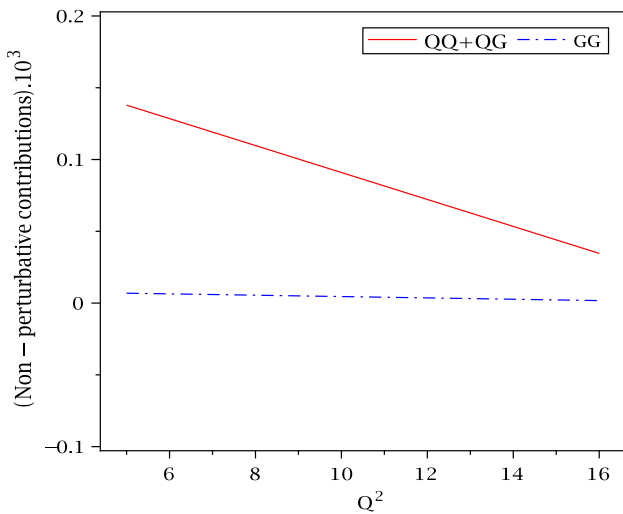


**Fig. 3** The quark–quark (QQ) plus quark–gluon (QG) condensate contributions (solid line) and also gluon–gluon (GG) condensate (dash-dot line) on  $Q^2$  for the off-shell  $D$  meson

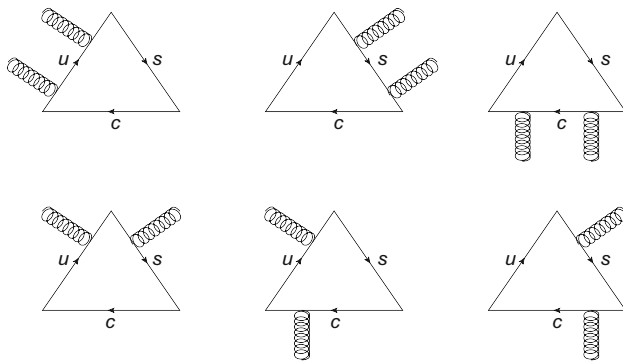


**Fig. 4** Non-perturbative diagrams for the off-shell  $K^*$  meson

and quark–gluon condensates since the heavy quark  $c$  is a spectator. Figure 4 shows these diagrams related to the gluon–gluon condensate.

After some straightforward but lengthy calculations and applying the double Borel transformations [19], the results for the gluon–gluon condensate contributions (Fig. 4), and quark–quark as well as quark–gluon contributions (Fig. 2) are obtained as

$$\Pi_{nonper}^{K^*} = -i \frac{C_{D_s DK^*}^{K^*}}{12} \left\langle \frac{\alpha_s}{\pi} G^2 \right\rangle, \quad \Pi_{nonper}^D = \frac{C_{D_s DK^*}^D}{12} \langle s\bar{s} \rangle, \tag{11}$$

where the explicit expressions for  $C_{D_s DK^*}^{K^*}$  and  $C_{D_s DK^*}^D$  are given in Appendix B. It should be noted that in order to obtain the gluon–gluon condensate contributions, we followed the same procedure as stated in Ref. [19].

The strong form factors are calculated by equating two representations of the correlation function and applying the Borel transformations [20] with respect to the  $p^2 (p^2 \rightarrow M_1^2)$

and  $p'^2 (p'^2 \rightarrow M_2^2)$  on the phenomenological as well as the perturbative and non-perturbative parts of the correlation function in order to suppress the contributions of the higher states and continuum. The equations for the strong form factors are obtained as follows:

$$g_{D_s DK^*}^{K^*}(q^2) = \Lambda_{D_s DK^*}^{K^*} \left\{ -\frac{1}{4\pi^2} \int_{(m_c+m_s)^2}^{s_0^{D_s}} ds' \int_{s_1}^{s_0^{D^*}} ds \rho_{D_s DK^*}^{K^*}(s, s', q^2) e^{-\frac{s}{M_1^2}} e^{-\frac{s'}{M_2^2}} - i \frac{M_1^2 M_2^2}{12} \left\langle \frac{\alpha_s}{\pi} G^2 \right\rangle \times C_{D_s DK^*}^{K^*} \right\},$$

$$g_{D_s DK^*}^D(q^2) = \Lambda_{D_s DK^*}^D \left\{ -\frac{1}{4\pi^2} \int_{(m_c+m_s)^2}^{s_0^{D_s}} ds' \int_{s_2}^{s_0^{K^*}} ds \rho_{D_s DK^*}^D(s, s', q^2) e^{-\frac{s}{M_1^2}} e^{-\frac{s'}{M_2^2}} + \frac{M_1^2 M_2^2}{12} \langle s\bar{s} \rangle \times C_{D_s DK^*}^D \right\}, \tag{12}$$

where  $\langle \frac{\alpha_s}{\pi} G^2 \rangle = 0.012 \text{ GeV}^4$  [21],  $\langle s\bar{s} \rangle = (0.8 \pm 0.2) \langle u\bar{u} \rangle$ , and  $\langle u\bar{u} \rangle = -(0.24 \pm 0.01 \text{ GeV})^3$  [22]. In these relations,  $s_0^{K^*}$  and  $s_0^{D^*}$  are the continuum thresholds in  $K^*$  and  $D(D_s)$  mesons, respectively. Also,  $s_1$  and  $s_2$  are the lower limits of the integrals over  $s$  as

$$s_1 = \frac{m_c^2(m_c^2 - s' + q^2)}{m_c^2 - s'}, \quad s_2 = \frac{m_s^2(m_s^2 - s' + q^2)}{m_s^2 - s'}.$$

The phrases  $\Lambda_{D_s DK^*}^{K^*}$  and  $\Lambda_{D_s DK^*}^D$  are defined as:

$$\Lambda_{D_s DK^*}^{K^*} = -\frac{m_c(m_c + m_s)(q^2 - m_{K^*}^2)}{m_{K^*} m_{D_s}^2 m_{D^*}^2 f_{K^*} f_{D_s} f_{D^*}} e^{\frac{m_D^2}{M_1^2}} e^{\frac{m_{D_s}^2}{M_2^2}},$$

$$\Lambda_{D_s DK^*}^D = -\frac{2 m_c(m_c + m_s) m_{K^*} (q^2 - m_D^2)}{m_D^2 m_{D_s}^2 f_{K^*} f_D f_{D_s} (q^2 - m_{D_s}^2 - m_{K^*}^2)} \times e^{\frac{m_{K^*}^2}{M_1^2}} e^{\frac{m_{D_s}^2}{M_2^2}}. \tag{13}$$

Following the previous steps, relations similar to Eq. (12) can be obtained for the strong form factors of the  $D_s D^* K^*$  vertex via the 3PSR. It should be noted that in this case, calculations are done for the Lorentz structure  $\epsilon^{\alpha\beta\mu\nu} p_\alpha p'_\beta$ . In order to have the correct relations for the strong form factors of the  $D_s D^* K^*$  vertex, the appropriate terms of  $\Lambda$ , the spectral density  $\rho$ , and quark–gluon condensate coefficients  $C_{D_s D^* K^*}^{K^*}$  and  $C_{D_s D^* K^*}^D$  should be replaced in Eq. (12). The explicit expressions for  $C_{D_s D^* K^*}^{K^*}$  and  $C_{D_s D^* K^*}^D$  are given in Appendix B. In addition, proper expressions for  $\Lambda$  related to the strong form factors  $g_{D_s D^* K^*}^{K^*}$  and  $g_{D_s D^* K^*}^D$  are as follows:

**Table 1** The leptonic decay constants in MeV

| $f_{K^*}$ [23] | $f_D$ [10]   | $f_{D_s}$ [24] | $f_{D^*}$ [25] |
|----------------|--------------|----------------|----------------|
| $220 \pm 5$    | $223 \pm 17$ | $294 \pm 27$   | $340 \pm 12$   |

$$\Lambda_{D_s D^* K^*}^{K^*} = -\frac{(m_c + m_s)(q^2 - m_{K^*}^2)}{m_{K^*} m_{D^*} m_{D_s}^2 f_{K^*} f_{D^*} f_{D_s}} e^{\frac{m_{D^*}^2}{M_1^2}} e^{\frac{m_{D_s}^2}{M_2^2}},$$

$$\Lambda_{D_s D^* K^*}^{D^*} = -\frac{(m_c + m_s)(q^2 - m_{D^*}^2)}{m_{K^*} m_{D^*} m_{D_s}^2 f_{K^*} f_{D^*} f_{D_s}} e^{\frac{m_{K^*}^2}{M_1^2}} e^{\frac{m_{D_s}^2}{M_2^2}}. \quad (14)$$

Also, the spectral densities are calculated as

$$\rho_{D_s D^* K^*}^{K^*} = -12I_0[C_1' m_c + C_2'(m_c - m_s) + m_c],$$

$$\rho_{D_s D^* K^*}^{D^*} = 12I_0[C_1 m_s + C_2(m_s - m_c) + m_s]. \quad (15)$$

### 3 Numerical analysis

In this section, the strong form factors and coupling constants for the  $D_s DK^*$  and  $D_s D^* K^*$  vertices as well as the branching ratio of the  $B^+ \rightarrow K^0 \pi^+$  decay are considered. For this aim, the values of quark and meson masses are chosen as:  $m_s = 0.14 \pm 0.01$  GeV,  $m_c = 1.26 \pm 0.02$  GeV,  $m_{D^*} = 2.01$  GeV,  $m_{K^*} = 0.89$  GeV,  $m_{D_s} = 1.97$  GeV, and  $m_D = 1.87$  GeV [23]. Moreover, the leptonic decay constants are presented in Table 1.

There are four auxiliary parameters containing the Borel mass parameters  $M_1$  and  $M_2$ , and continuum thresholds  $s_0^{K^*}$ ,  $s_0^{D(D_s)}$  and  $s_0^{D^*}$  in Eq. (12). The strong form factors and coupling constants are the physical quantities, and should be independent of them. However the continuum thresholds are not completely arbitrary; these are related to the energy of the first excited state. The values of the continuum thresholds are taken to be  $s_0^{K^*} = (m_{K^*} + \delta)^2$ ,  $s_0^{D(D_s)} = (m_{D(D_s)} + \delta')^2$  and  $s_0^{D^*} = (m_{D^*} + \delta')^2$ . We use  $0.40 \text{ GeV} \leq \delta \leq 0.60 \text{ GeV}$  and  $0.30 \text{ GeV} \leq \delta' \leq 0.70 \text{ GeV}$  [2–4]. Our results should be almost insensitive to the intervals of the Borel parameters. On the other hand, the intervals of the Borel mass parameters must suppress the higher states, continuum and contributions of the highest-order operators. In other words, the sum rule for the strong form factors must converge. We get a very good stability for the form factors as a function of the two independent Borel parameters in the regions  $6 \text{ GeV}^2 < M_1^2 < 8 \text{ GeV}^2$  and  $6 \text{ GeV}^2 < M_2^2 < 8 \text{ GeV}^2$  when  $K^*$  is an off-shell meson, and also  $6 \text{ GeV}^2 < M_1^2 < 8 \text{ GeV}^2$  and  $8 \text{ GeV}^2 < M_2^2 < 10 \text{ GeV}^2$  when  $D$  ( $D^*$ ) meson is an off-shell. Figure 5 shows the dependence of the form factors  $g_{D_s DK^*}^{K^*}$  and  $g_{D_s DK^*}^D$  on the Borel mass parameters  $M_1^2$  and  $M_2^2$  for three values of the continuum thresholds  $s_0^{K^*}$  and  $s_0^D$ .

As previously mentioned, these intervals of  $M_1^2$  and  $M_2^2$  must suppress the higher states, continuum and contributions

of the highest-order operators. For instance, Fig. 6 shows the strong form factor  $g_{D_s DK^*}^D$  with respect to  $Q^2$  for different values of the Borel parameters. In addition, this figure displays perturbative contribution of the form factor  $g_{D_s DK^*}^D$ . As can be seen, the important contribution of the form factor comes from the perturbative part, i.e., the contributions of the quark–quark and quark–gluon condensates, as the most important terms of the condensates in this case, are less than the perturbative part. Therefore, the obtained regions for the Borel parameters can suppress the higher order condensates.

It should be noted that, from now on, to calculate the strong form factors  $g_{D_s DK^*}^{K^*}$  and  $g_{D_s D^* K^*}^{K^*}$ , we get  $[M_1^2, M_2^2] = [7, 7] \text{ GeV}^2$ , and for  $g_{D_s DK^*}^D$  and  $g_{D_s D^* K^*}^D$ , we get  $[M_1^2, M_2^2] = [7, 9] \text{ GeV}^2$ .

The numerical results for the strong form factors calculated via the 3PSR in Eq. (12) have a cut-off. Therefore, we look for a parametrization of the form factors in such that in the validity region of the 3PSR, this parametrization coincides with the sum rules prediction. Our numerical calculations show that the sum rule predictions for the form factors in Eq. (12) are well fitted to the following function:

$$g(Q^2) = A e^{-Q^2/B}.$$

The values of the parameters  $A$  and  $B$  are given in Table 2 for various  $(\delta, \delta')$ .

The dependence of the strong form factors  $g_{D_s DK^*}^D(Q^2)$ ,  $g_{D_s DK^*}^{K^*}(Q^2)$ ,  $g_{D_s D^* K^*}^{D^*}(Q^2)$  and  $g_{D_s D^* K^*}^{K^*}(Q^2)$  in  $Q^2$  are shown in Fig. 7. The boxes and circles in Fig. 7 show the results of the numerical evaluation via the 3PSR for the form factors  $g_{D_s DK^*}^{K^*}(g_{D_s D^* K^*}^{K^*})$  and  $g_{D_s DK^*}^D(g_{D_s D^* K^*}^D)$ , respectively. As can be seen, the form factors and their fit functions coincide together, well.

The value of the strong form factors at  $Q^2 = -m_m^2$ , where  $m_m$  is the mass of the off-shell meson, is defined as coupling constant. Coupling constant results of the two vertices,  $D_s DK^*$  and  $D_s D^* K^*$ , are presented in Table 3. It should be mentioned that the coupling constant  $g_{D_s DK^*}$  is the dimensionless quantity and the coupling constant  $g_{D_s D^* K^*}$  is in the unit of  $\text{GeV}^{-1}$ . The errors are estimated by variation of the Borel parameters, variation of the continuum thresholds, the leptonic decay constants and uncertainties in the values of the other input parameters. It should be noted that the main uncertainty comes from the continuum thresholds and the decay constants.

Table 4 shows a comparison between our results with the values predicted by the light-cone sum rules (LCSR) method. The results of Ref. [26] have been rescaled according to the strong form factor definitions in Eq. (2). It should be reminded that the value of  $g_{D_s DK^*}(g_{D_s D^* K^*})$  in Table 4 is an average of the two coupling constant values  $g_{D_s DK^*}^{K^*}(g_{D_s D^* K^*}^{K^*})$  and  $g_{D_s DK^*}^D(g_{D_s D^* K^*}^D)$  in Table 3.



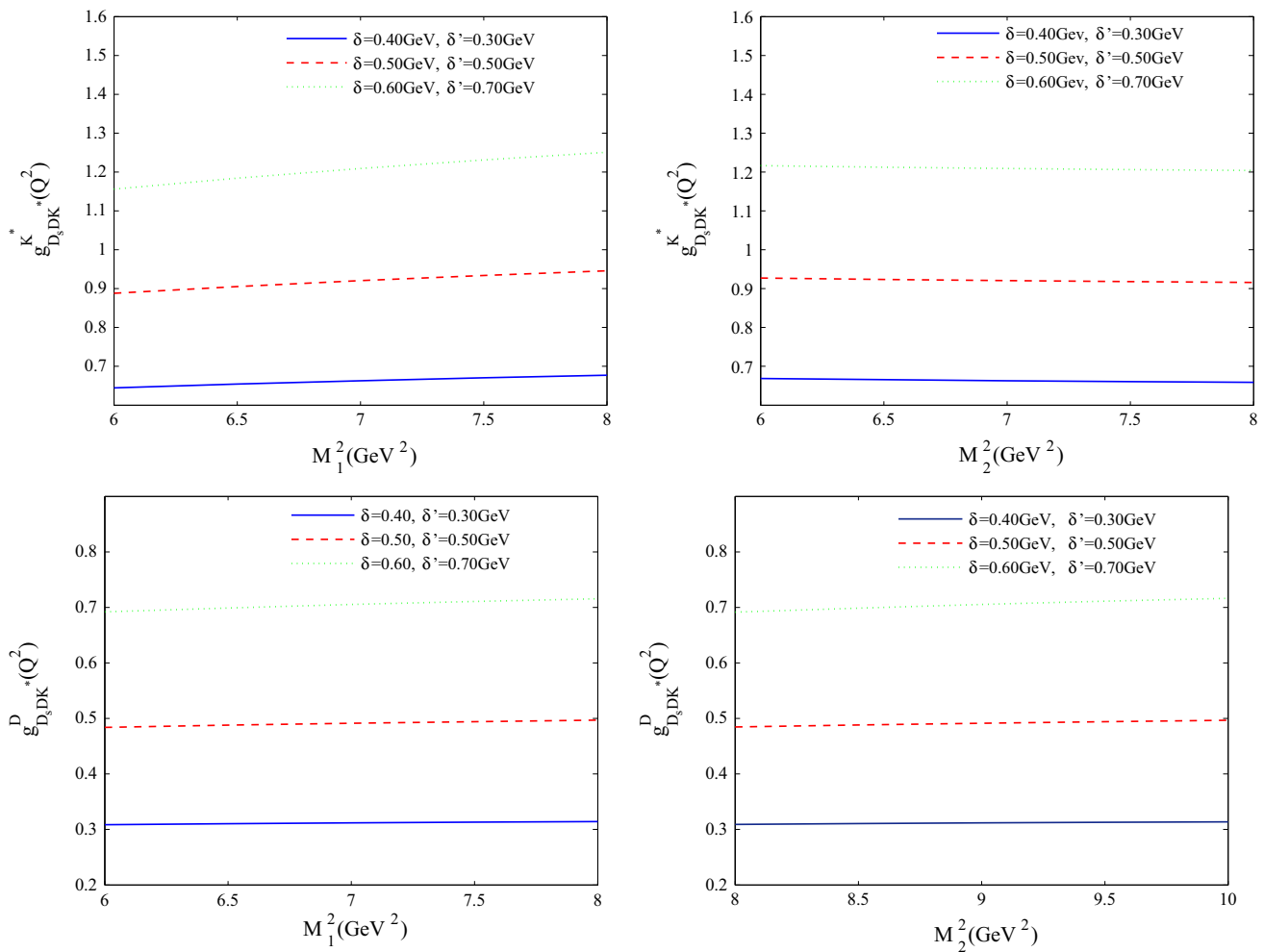


**Fig. 5**  $M_1^2$  and  $M_2^2$  dependence of  $g_{D_s DK^*}^{K^*}$  and  $g_{D_s DK^*}^D$  for three values of the continuum thresholds

In order to investigate the strong coupling constant values via the  $SU_f(3)$  symmetry, the mass of the  $s$  quark is ignored in all calculations. In view of the  $SU_f(3)$  symmetry, the values of the parameters  $A$  and  $B$  for the  $g_{D_s DK^*}$  and  $g_{D_s D^* K^*}$  strong form factors are given in Table 5 with  $(\delta, \delta') = (0.50, 0.50)$  GeV. In addition, considering the  $SU_f(3)$  symmetry, we obtain the values of the coupling constants of the vertices  $D_s DK^*$  and  $D_s D^* K^*$  as shown in Table 6. It is possible to compare the coupling constant values of  $g_{D_s DK^*}$  and  $g_{D_s D^* K^*}$  with  $g_{DD\rho}$  and  $g_{D^* D^* \rho}$  respectively, in the  $SU_f(3)$  symmetry consideration. Table 7 shows a comparison between our results with the values predicted by the LCSR and 3PSR methods.

An example of specific application of these coupling constants is in branching ratio calculations of  $B$  meson decays. It is reminded that re-scattering effects play an important role in the hadronic  $B$  decays. It is not easy to take them into account in a systematic way due to the non-perturbative nature of the multi-particle dynamics. In practical calculations, the phe-

nomenological models can be used to overcome the difficulty [26]. The one-particle-exchange is one of these phenomenological models. In this model, the soft re-scattering of the intermediate states in two-body channels with one-particle exchange makes the main contributions. The phenomenological Lagrangian contains many input parameters, which describe the strong couplings among the charmed mesons in the hadronic  $B$  decays.

For instance, we would like to consider the branching ratio of the  $B^+ \rightarrow K^{*0} \pi^+$  decay according to the method of Refs. [27,28]. It should be noted that our main goal in this investigation is to illustrate the use of the coupling constants  $g_{D_s DK^*}$  and  $g_{D_s D^* K^*}$  in branching ratio calculations of  $B$  decays. Therefore, we do not discuss the methods of calculation, which are presented here.

According to Refs. [27,28], the  $B \rightarrow K^* \pi$  decay amplitude,  $A_{K^* \pi}$  contains the short-distance (SD) and the long-distance (LD) contributions:

$$\mathcal{M}_{K^* \pi} = \mathcal{M}_{SD} + \mathcal{M}_{LD}. \tag{16}$$

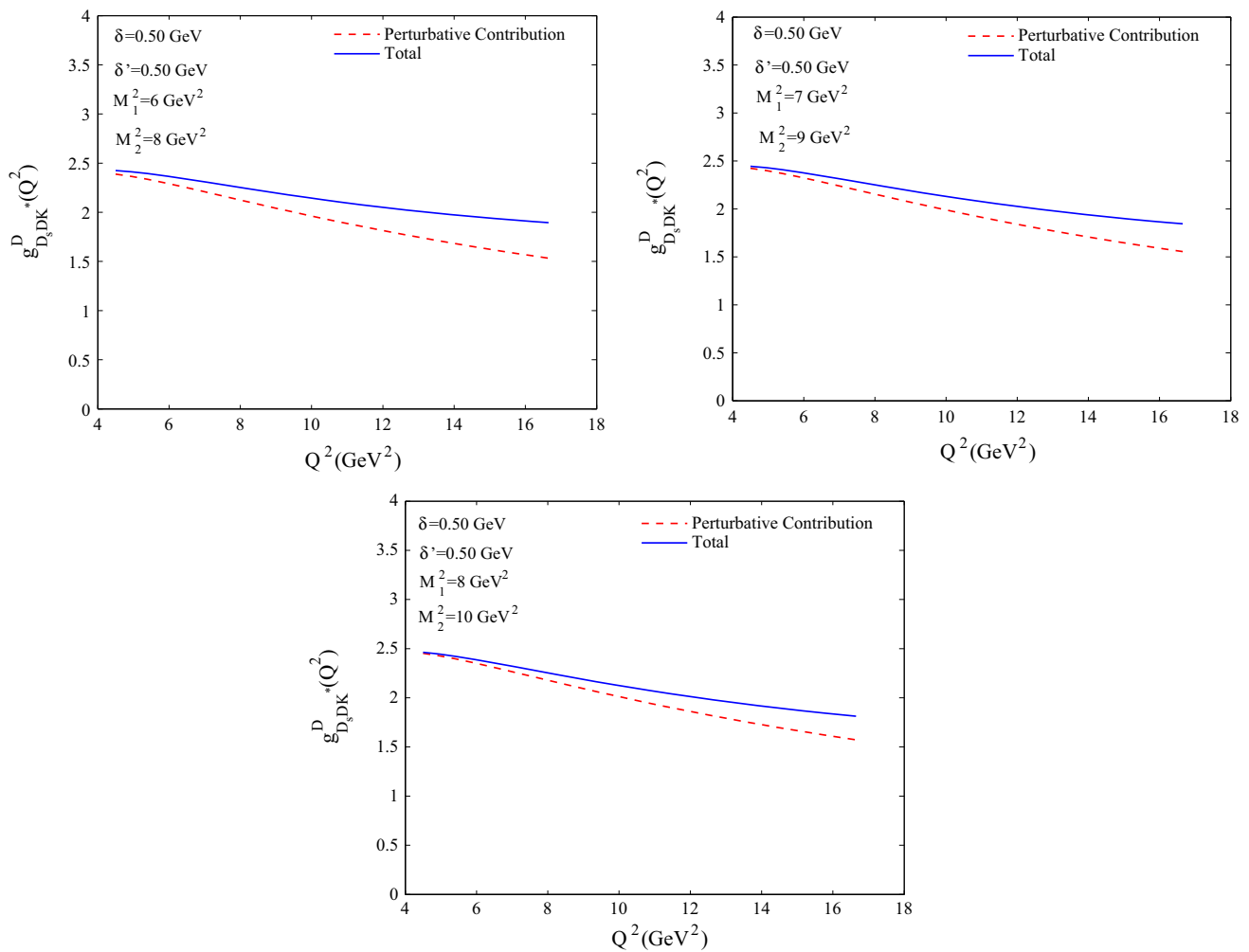


**Fig. 6** The strong form factor  $g_{D_s DK}^D$  on  $Q^2$  for different values of the Borel parameters

**Table 2** Parameters appearing in the fit functions for the  $D_s DK^*$  and  $D_s D^* K^*$  vertices for various  $(\delta, \delta')$ , where  $(\delta_1, \delta'_1) = (0.40, 0.30)$ ,  $(\delta_2, \delta'_2) = (0.50, 0.50)$  and  $(\delta_3, \delta'_3) = (0.60, 0.70)$  GeV

| Form factor                  | $A(\delta_1, \delta'_1)$ | $B(\delta_1, \delta'_1)$ | $A(\delta_2, \delta'_2)$ | $B(\delta_2, \delta'_2)$ | $A(\delta_3, \delta'_3)$ | $B(\delta_3, \delta'_3)$ |
|------------------------------|--------------------------|--------------------------|--------------------------|--------------------------|--------------------------|--------------------------|
| $g_{D_s DK^*}^{K^*}(Q^2)$    | 1.58                     | 2.00                     | 1.97                     | 2.86                     | 2.41                     | 4.15                     |
| $g_{D_s DK^*}^D(Q^2)$        | 2.29                     | 29.07                    | 2.81                     | 37.62                    | 3.11                     | 27.12                    |
| $g_{D_s D^* K^*}^{K^*}(Q^2)$ | 2.75                     | 9.82                     | 3.19                     | 5.41                     | 4.21                     | 14.71                    |
| $g_{D_s D^* K^*}^{D^*}(Q^2)$ | 3.31                     | 52.77                    | 3.73                     | 43.05                    | 4.23                     | 32.05                    |

Using the effective Hamiltonian for non-leptonic  $B$  decays [29–33] in the factorization approximation, the value of the SD amplitude is  $\mathcal{M}_{SD} = 1.52 \times 10^{-8}$ , which is evaluated by the following formula [27]:

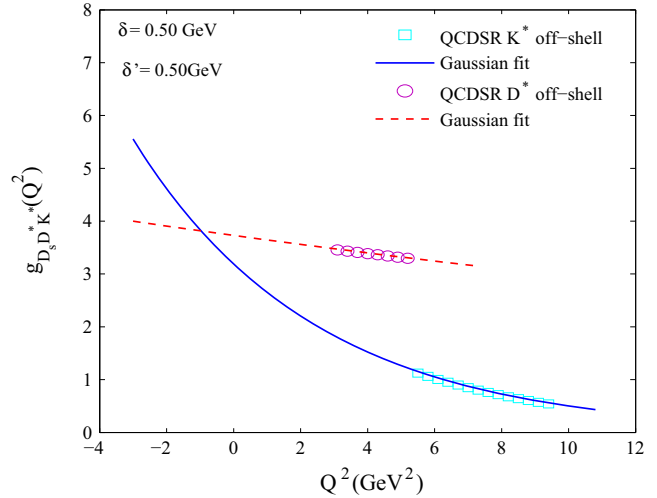
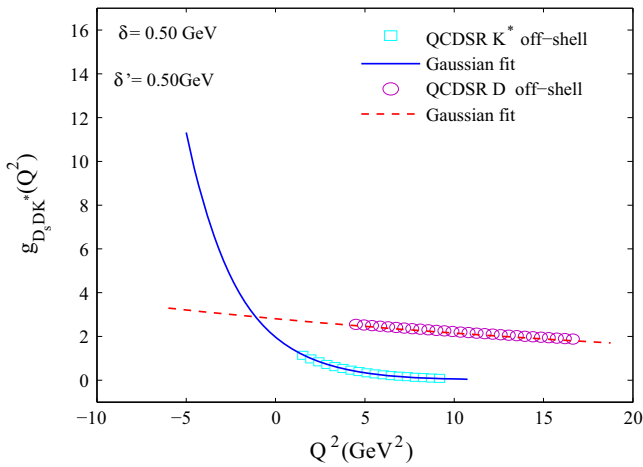
$$\begin{aligned}
 \mathcal{M}_{SD}(B^+ \rightarrow K^{*0} \pi^+) &= G_F \sqrt{2} F_1^{B \rightarrow \pi}(m_{K^*}^2) f_{K^*} m_{K^*} V_{tb}^* V_{ts} \\
 &\times \left[ a_4 - \frac{a_{10}}{2} \right] (\varepsilon^* \cdot p_B). \tag{17}
 \end{aligned}$$

Figure 8 shows diagrams, for the  $B \rightarrow K^* \pi$  decay with  $D_s, D^*$  intermediate states, used to calculate the  $\mathcal{M}_{LD}$  part of

the amplitude. As can be seen in Fig. 8, the  $B \rightarrow K^* \pi$  decay may be occur in two steps. First, the  $B$  decays into a  $D_s D^*$  intermediate state ( $B \rightarrow D_s D^*$ ), and then these two particles exchange a  $D(D^*)$  producing the final  $K^*$  and  $\pi$ . In order to compute the effect of these interactions in the final decay rate, we need the  $D_s DK^*(D_s D^* K^*)$  and  $D^* D \pi(D^* D^* \pi)$  form factors.

The  $\mathcal{M}_{LD}$  consists of two parts, real and imaginary:  $\mathcal{M}_{LD} = \mathcal{R}_{LD} + i \mathcal{I}_{LD}$ . (18)

The computation of the imaginary part of the charming penguin diagrams contributing to  $B \rightarrow K^* \pi$  decay gives



**Fig. 7** The strong form factors  $g_{D_s DK^*}^D, g_{D_s DK^*}^{K^*}, g_{D_s D^* K^*}^D$  and  $g_{D_s D^* K^*}^{K^*}$  on  $Q^2$

**Table 3** The coupling constant of the vertices  $D_s DK^*$  and  $D_s D^* K^*$

|                   | Off-shell charmed | Off-shell $K^*$ |
|-------------------|-------------------|-----------------|
| $g_{D_s DK^*}$    | $3.09 \pm 0.50$   | $2.60 \pm 0.42$ |
| $g_{D_s D^* K^*}$ | $4.10 \pm 0.67$   | $3.70 \pm 0.61$ |

**Table 4** Values of the strong coupling constant using the 3PSR (ours) and LCSR approaches

| $g$               | Ours            | LCSR [26]       |
|-------------------|-----------------|-----------------|
| $g_{D_s DK^*}$    | $2.85 \pm 0.46$ | $3.22 \pm 0.32$ |
| $g_{D_s D^* K^*}$ | $3.90 \pm 0.64$ | $4.04 \pm 0.74$ |

**Table 5** Parameters appearing in the fit functions for the  $g_{D_s DK^*}$  and  $g_{D_s D^* K^*}$  form factors in  $SU_f(3)$  symmetry with  $(\delta, \delta') = (0.50, 0.50)$  GeV

| Form factor                  | $A$  | $B$   |
|------------------------------|------|-------|
| $g_{D_s DK^*}^{K^*}(Q^2)$    | 2.08 | 2.53  |
| $g_{D_s DK^*}^D(Q^2)$        | 2.61 | 37.16 |
| $g_{D_s D^* K^*}^{K^*}(Q^2)$ | 2.60 | 5.04  |
| $g_{D_s D^* K^*}^D(Q^2)$     | 2.88 | 24.09 |

**Table 6** The coupling constants of the vertices  $D_s DK^*$  and  $D_s D^* K^*$ , in  $SU_f(3)$  symmetry

|                   | Off-shell charmed | Off-shell $K^*$ |
|-------------------|-------------------|-----------------|
| $g_{D_s DK^*}$    | $2.87 \pm 0.47$   | $2.84 \pm 0.46$ |
| $g_{D_s D^* K^*}$ | $3.40 \pm 0.55$   | $3.04 \pm 0.49$ |

$$\mathcal{I}_{LD} = \frac{m_D}{32\pi^2 m_B} \sqrt{\omega^{*2} - 1} \int d\mathbf{n} \mathcal{M}(B \rightarrow D_s D^*) \times \mathcal{M}(D_s D^* \rightarrow K^* \pi), \quad (19)$$

**Table 7** Values of the coupling constant using the LCSR, and 3PSR

| $g$               | Ours            | 3PSR [5–7]      | LCSR [26]       |
|-------------------|-----------------|-----------------|-----------------|
| $g_{D_s DK^*}$    | $2.86 \pm 0.46$ | $3.42 \pm 0.44$ | $2.62 \pm 0.66$ |
| $g_{D_s D^* K^*}$ | $3.22 \pm 0.52$ | $4.11 \pm 0.44$ | $3.56 \pm 0.60$ |

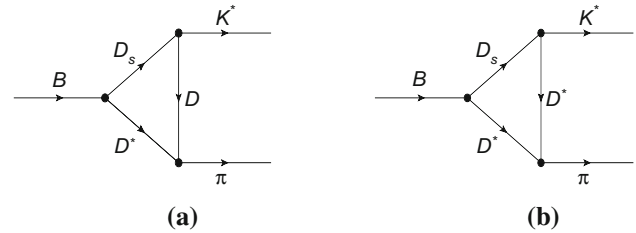


**Fig. 8** Diagrams for the  $B \rightarrow K^* \pi$  decay with  $D_s, D^*$  intermediate states

where the integration is over the solid angle. Using the following kinematics:

$$p_B^\mu = m_B v^\mu = (m_B, \vec{0}), \quad p_{D^*}^\mu = m_{D^*} v'^\mu, \quad q = p_B - p_{D^*}, \quad (20)$$

the amplitude for the decay  $B \rightarrow D_s D^*$  is computed by factorization as:

$$\mathcal{M}(B(v) \rightarrow D_s(q) D^*(\epsilon, v')) = -K (m_B + m_{D^*}) \epsilon^* \cdot v, \quad (21)$$

where  $K = \sqrt{2} \frac{G_F}{1+\omega^*} V_{cb}^* V_{cs} a_2 \sqrt{m_B m_{D^*}} f_{D_s}$ , and  $\omega^* = \frac{m_B^2 + m_{D^*}^2 - m_{D_s}^2}{2m_{D^*} m_B}$ . Using the heavy quark effective lagrangian, the calculation of the amplitude  $D_s D^* \rightarrow K^* \pi$  leads to [27]:



$$\begin{aligned} & \mathcal{M}(D_s(q)D^*(\epsilon, v') \rightarrow K^*(p_K, \hat{\epsilon})\pi(p_\pi)) \\ &= -\frac{2g F^2(|\mathbf{p}_\pi|) g_V}{f_\pi} \frac{g_V}{\sqrt{2}} \sqrt{\frac{m_{D^*}}{m_{D_s}}} \epsilon_\lambda \hat{\epsilon}_\sigma^* \\ & \times \left[ \frac{2\beta m_D q^\sigma p_\pi^\lambda}{(m_D v' - p_\pi)^2 - m_D^2} \right. \\ & \left. + \frac{4\lambda m_{D^*} G^{\sigma\lambda}(p_\pi, p_K, v')}{(m_{D^*} v' - p_\pi)^2 - m_{D^*}^2} \right], \end{aligned} \tag{22}$$

where

$$\begin{aligned} G^{\sigma\lambda}(p_\pi, p_K, v') &= -(v' \cdot q) \left( g^{\sigma\lambda}(p_K \cdot p_\pi) - p_\pi^\sigma p_K^\lambda \right) \\ & - (q \cdot p_\pi) \left( v'^\sigma p_K^\lambda - g^{\sigma\lambda}(v' \cdot p_K) \right) \\ & - q^\lambda \left( p_\pi^\sigma (p_K \cdot v') - v'^\sigma (p_K \cdot p_\pi) \right). \end{aligned} \tag{23}$$

Eq. (22) is calculated based on the three parameters  $F(|\mathbf{p}_\pi|)$ ,  $g$  and  $g_V$ .  $F(|\mathbf{p}_\pi|)$  is a form factor taking into account that in the vertex  $DD^*\pi$  the pion is not soft and therefore the coupling constant should be corrected. Its central value is  $F(|\mathbf{p}_\pi|) = 0.065$  determined by a quark potential model and discussed in Ref. [28]. The definition of  $g$  is related to the coupling  $G_{D^*D\pi}$ , which can be written in general as  $G_{D^*D\pi} = \frac{2g m_D}{f_\pi}$ . The parameter  $g$  is predicted to have the value  $g = 0.59 \pm 0.07 \pm 0.01$  [35]. The definition of  $g_V$  is expressed in Ref. [34] and its value is  $g_V \simeq 5.8$ . The basic parameters  $\beta$  and  $\lambda$  in the heavy quark effective Lagrangian can be related to the strong coupling constants  $g_{D_s DK^*}$  and  $g_{D_s D^* K^*}$  as [1, 26]:

$$\beta = \frac{\sqrt{2} g_{D_s DK^*}}{2 g_V}, \quad \lambda = \frac{\sqrt{2} g_{D_s D^* K^*}}{2 g_V}. \tag{24}$$

Our numerical values for the  $g_{D_s DK^*}$  and  $g_{D_s D^* K^*}$  have been presented in Table 4. Using Eqs. (21) and (22) in Eq. (19) and straightforward calculations, our numerical value for the imaginary part of the LD amplitude of two diagrams (a) and (b) in Fig. 8 is  $\mathcal{I}_{LD}^{(a,b)} = -2.46 \times 10^{-8}$ .

A similar method of the imaginary part is used to calculate the real part of the LD amplitude [27]. The result for  $\mathcal{R}_{LD}^{(a,b)} = 2.34 \times 10^{-8}$ , which is the same order of the imaginary part.

The branching ratio of the non-leptonic process  $B^+ \rightarrow K^{*0}\pi^+$  is given by

$$\begin{aligned} & \mathcal{BR}(B^+ \rightarrow K^{*0}\pi^+) \\ &= \frac{\tau_B}{16\pi m_B^3} |\mathcal{M}_{K^*\pi}|^2 \sqrt{\lambda(m_B^2, m_K^2, m_\pi^2)}, \end{aligned} \tag{25}$$

where  $\lambda(m_B^2, m_K^2, m_\pi^2) = m_B^4 + m_K^4 + m_\pi^4 - 2m_B^2 m_K^2 - 2m_B^2 m_\pi^2 - 2m_K^2 m_\pi^2$ . Our results for the branching ratio of the  $B^+ \rightarrow K^{*0}\pi^+$  decay are presented in Table 8. These results are obtained for only the short distance amplitude

**Table 8** Branching ratio values (units  $10^{-5}$ ) of the  $B^+ \rightarrow K^{*0}\pi^+$  mode

|   | $\mathcal{M}_{SD}$ | $\mathcal{M}_{SD} + \mathcal{M}_{LD}$ | Exp[36,37]      |
|---|--------------------|---------------------------------------|-----------------|
| $\mathcal{BR}(B^+ \rightarrow K^{*0}\pi^+)$ | $0.21 \pm 0.07$    | $1.62 \pm 0.41$                       | $1.21 \pm 0.31$ |

( $\mathcal{M}_{SD}$ ), and also for the total amplitude ( $\mathcal{M}_{SD} + \mathcal{M}_{LD}$ ). Furthermore, this table contains the experimental value for the branching ratio of the  $B^+ \rightarrow K^{*0}\pi^+$ . Considering the error in the experimental value, our estimation for the branching ratio value of the  $B^+ \rightarrow K^{*0}\pi^+$  decay with the total amplitude is in consistent agreement with the experimental data.

In summary, taking into account the contributions of the quark–quark, quark–gluon and gluon–gluon condensate corrections, the strong form factors  $g_{D_s DK^*}$  and  $g_{D_s D^* K^*}$  were estimated within the 3PSR with and without the  $SU_f(3)$  symmetry. A comparison was made between our results and the predictions of other methods. Finally, the branching ratio of the  $B^+ \rightarrow K^{*0}\pi^+$  decay was estimated using the coupling constants of the  $D_s DK^*$  and  $D_s D^* K^*$  vertices.

**Acknowledgements** Partial support from the Isfahan University of Technology research council is appreciated.

**Open Access** This article is distributed under the terms of the Creative Commons Attribution 4.0 International License (<http://creativecommons.org/licenses/by/4.0/>), which permits unrestricted use, distribution, and reproduction in any medium, provided you give appropriate credit to the original author(s) and the source, provide a link to the Creative Commons license, and indicate if changes were made. Funded by SCOAP<sup>3</sup>.

### Appendix A

In this appendix, the explicit expressions of the coefficients in the spectral densities are given as:

$$\begin{aligned} I_0(s, s', q^2) &= \frac{1}{4\lambda^{\frac{1}{2}}(s, s', q^2)}, \\ \lambda(a, b, c) &= a^2 + b^2 + c^2 - 2ac - 2bc - 2ab, \\ \Delta &= s' + m_s^2 - m_c^2, \\ \Delta' &= s' + m_c^2 - m_s^2, \\ \Delta'' &= s + m_s^2, \\ u &= s + s' - q^2, \\ C_1 &= \frac{1}{\lambda(s, s', q^2)} [2s'\Delta'' - u\Delta], \\ C_2 &= \frac{1}{\lambda(s, s', q^2)} [2s\Delta - u\Delta''], \end{aligned}$$

also  $C'_1 = C_1|_{m_c \leftrightarrow m_s}$  and  $C'_2 = C_2|_{m_c \leftrightarrow m_s}$ .

**Appendix B**

In this appendix, the explicit expressions of the coefficients of the quark and gluon condensate contributions of the strong form factor in the Borel transform scheme is presented.

$$C_{D_s DK^*}^D = \left( 3 \frac{m_s m_c^2}{M_1^4 M_2^2} - 3 \frac{m_s q^2}{M_1^4 M_2^2} + 3 \frac{m_c m_s^2}{M_1^4 M_2^2} - \frac{5}{2} \frac{m_0^2 m_c}{M_1^4 M_2^2} + 3 \frac{m_s m_c^2}{M_1^2 M_2^4} - 3 \frac{m_0^2 m_c}{M_1^2 M_2^4} - \frac{1}{2} \frac{m_0^2 m_c^3}{M_1^4 M_2^4} + \frac{1}{2} \frac{m_0^2 m_c q^2}{M_1^4 M_2^4} + 3 \frac{m_c^3 m_s^2}{M_1^2 M_2^6} - \frac{3}{2} \frac{m_0^2 m_c^3}{M_1^2 M_2^6} \right) \times e^{-\frac{m_c^2}{M_2^2}},$$

$$C_{D_s D^* K^*}^{D^*} = \left( 6 \frac{m_s m_c}{M_1^2 M_2^4} - 6 \frac{q^2 m_s^2}{M_1^4 M_2^4} + 2 \frac{m_0^2 q^2}{M_1^4 M_2^4} + 6 \frac{m_c^2 m_s^2}{M_1^4 M_2^4} - 2 \frac{m_0^2 m_c^2}{M_1^4 M_2^4} + 6 \frac{m_c^2 m_s^2}{M_1^2 M_2^6} - 3 \frac{m_0^2 m_c^2}{M_1^2 M_2^6} \right) \times e^{-\frac{m_c^2}{M_2^2}},$$

$$C_{D_s DK^*}^{K^*} = -\hat{I}_0(3, 2, 2)m_c^6 - \hat{I}_1(3, 2, 2)m_c^5 m_s + \hat{I}_2(3, 2, 2)m_c^5 m_s + 2\hat{I}_0(3, 2, 2)m_c^5 m_s - \hat{I}_1(3, 2, 2)m_c^4 m_s^2 + \hat{I}_2(3, 2, 2)m_c^4 m_s^2 - 2\hat{I}_0(3, 2, 2)m_c^3 m_s^3 - \hat{I}_2(3, 1, 2)m_c^4 - \hat{I}_0^{[0,1]}(3, 2, 2)m_c^4 + 3\hat{I}_1(2, 2, 2)m_c^4 - 3\hat{I}_2(2, 2, 2)m_c^4 + \hat{I}_1(3, 1, 2)m_c^4 - 3\hat{I}_0(3, 2, 1)m_c^4 + 2\hat{I}_2(2, 2, 2)m_c^3 m_s + 2\hat{I}_0(3, 2, 1)m_c^3 m_s + 2\hat{I}_0^{[1,0]}(3, 2, 2)m_c^3 m_s - 2\hat{I}_1(2, 2, 2)m_c^3 m_s + \hat{I}_2^{[1,0]}(3, 2, 2)m_c^3 m_s + 6\hat{I}_0(4, 1, 1)m_c^3 m_s + 4\hat{I}_0(2, 2, 2)m_c^3 m_s + \hat{I}_2(3, 2, 1)m_c^3 m_s - \hat{I}_1(3, 2, 1)m_c^3 m_s + \hat{I}_0(3, 1, 2)m_c^3 m_s + \hat{I}_1^{[1,0]}(3, 2, 2)m_c^3 m_s - 2\hat{I}_0(2, 2, 2)m_c^2 m_s^2 + 2\hat{I}_1(3, 1, 2)m_c^2 m_s^2 - 3\hat{I}_0(4, 1, 1)m_c^2 m_s^2 - 2\hat{I}_2(3, 1, 2)m_c^2 m_s^2 - 2\hat{I}_0^{[0,1]}(3, 2, 2)m_c^2 m_s^2 + 5\hat{I}_0(3, 1, 2)m_c m_s^3 + 2\hat{I}_2(2, 1, 3)m_c m_s^3 + 2\hat{I}_2(3, 1, 2)m_c m_s^3 - 2\hat{I}_1(2, 1, 3)m_c m_s^3 - 2\hat{I}_1(3, 1, 2)m_c m_s^3 - \hat{I}_0(2, 2, 2)m_s^4 + \hat{I}_0^{[1,0]}(3, 2, 2)m_s^4 - 5\hat{I}_1^{[1,1]}(3, 2, 2)m_c^2 + 2\hat{I}_0^{[0,1]}(3, 1, 2)m_c^2 - 5\hat{I}_2^{[1,1]}(3, 2, 2)m_c^2 + 3\hat{I}_2^{[1,0]}(3, 2, 1)m_c^2 + 2\hat{I}_0^{[0,1]}(2, 2, 2)m_c^2 + 3\hat{I}_1(1, 3, 1)m_c^2 - 2\hat{I}_0(1, 2, 2)m_c^2 + 3\hat{I}_1^{[1,0]}(3, 2, 1)m_c^2$$

$$-3\hat{I}_2(1, 3, 1)m_c^2 - 12\hat{I}_0(1, 1, 3)m_c m_s + \hat{I}_2^{[1,1]}(3, 2, 2)m_c m_s - 3\hat{I}_1^{[1,0]}(3, 2, 1)m_c m_s - 9\hat{I}_0(2, 1, 2)m_c m_s + 3\hat{I}_1(1, 3, 1)m_c m_s - 2\hat{I}_1^{[0,1]}(2, 1, 3)m_c m_s - \hat{I}_2(2, 2, 1)m_c m_s - 3\hat{I}_2^{[1,0]}(3, 2, 1)m_c m_s + \hat{I}_1(2, 2, 1)m_c m_s + 4\hat{I}_1(2, 1, 2)m_c m_s - 2\hat{I}_2^{[0,1]}(2, 1, 3)m_c m_s - 4\hat{I}_2(2, 1, 2)m_c m_s - 3\hat{I}_2(1, 3, 1)m_c m_s + \hat{I}_1^{[1,1]}(3, 2, 2)m_c m_s - 2\hat{I}_0(3, 1, 1)m_s^2 + \hat{I}_2(2, 1, 2)m_s^2 - \hat{I}_1(2, 1, 2)m_s^2 + 2\hat{I}_0^{[1,0]}(2, 2, 2)m_s^2 + 3\hat{I}_0(1, 1, 3)m_s^2 + \hat{I}_2^{[1,0]}(2, 2, 2)m_s^2 - 2\hat{I}_0(2, 2, 1)m_s^2 + \hat{I}_1^{[1,0]}(2, 2, 2)m_s^2 + 2\hat{I}_0^{[0,1]}(2, 2, 2)m_s^2 + 3\hat{I}_0(2, 1, 2)m_s^2 - 2\hat{I}_0^{[1,1]}(2, 2, 2) - 2\hat{I}_0^{[0,2]}(3, 1, 2) - 2\hat{I}_1(1, 2, 1) + 2\hat{I}_0^{[0,1]}(2, 2, 1) + \hat{I}_0^{[0,1]}(1, 2, 2) + 2\hat{I}_2(1, 2, 1) - 3\hat{I}_0^{[1,1]}(3, 2, 1) - 3\hat{I}_0^{[0,1]}(1, 1, 3) + \hat{I}_0(2, 1, 1) + 2\hat{I}_2(1, 1, 2) + \hat{I}_0^{[0,1]}(2, 1, 2) - 2\hat{I}_1(1, 1, 2),$$

$$C_{D_s D^* K^*}^{K^*} = 2\hat{I}_2(3, 2, 2)m_c^5 + 2\hat{I}_0(3, 2, 2)m_c^5 + 2\hat{I}_1(3, 2, 2)m_c^5 - 2\hat{I}_2(3, 2, 2)m_c^4 m_s - 2\hat{I}_0(3, 2, 2)m_c^3 m_s^2 - 2\hat{I}_2(3, 2, 2)m_c^3 m_s^2 - 2\hat{I}_1(3, 2, 2)m_c^3 m_s^2 + 2\hat{I}_2(3, 2, 2)m_c^3 m_s^3 + 4\hat{I}_2(2, 2, 2)m_c^3 + 2\hat{I}_0^{[0,1]}(3, 2, 2)m_c^3 + 6\hat{I}_1(4, 1, 1)m_c^3 + 2\hat{I}_2^{[1,0]}(3, 2, 2)m_c^3 + 6\hat{I}_0(4, 1, 1)m_c^3 + 4\hat{I}_0(2, 2, 2)m_c^3 + 2\hat{I}_0(3, 2, 1)m_c^3 + 2\hat{I}_0^{[1,0]}(3, 2, 2)m_c^3 + 2\hat{I}_1^{[0,1]}(3, 2, 2)m_c^3 + 2\hat{I}_2^{[0,1]}(3, 2, 2)m_c^3 - 2\hat{I}_1(3, 1, 2)m_c^3 + 2\hat{I}_1(3, 2, 1)m_c^3 + 2\hat{I}_1^{[1,0]}(3, 2, 2)m_c^3 + 4\hat{I}_1(2, 2, 2)m_c^3 + 6\hat{I}_2(4, 1, 1)m_c^3 - 4\hat{I}_2(2, 2, 2)m_c^2 m_s - 2\hat{I}_2^{[1,0]}(3, 2, 2)m_c^2 m_s + 8\hat{I}_0(2, 1, 3)m_c^2 m_s + 2\hat{I}_1(3, 1, 2)m_c^2 m_s - 2\hat{I}_0(3, 1, 2)m_c^2 m_s + 4\hat{I}_2(2, 1, 3)m_c^2 m_s - 2\hat{I}_2(3, 1, 2)m_c^2 m_s - 6\hat{I}_2(4, 1, 1)m_c^2 m_s - 2\hat{I}_2^{[0,1]}(3, 2, 2)m_c^2 m_s + 4\hat{I}_1(3, 1, 2)m_c m_s^2 + 4\hat{I}_0(3, 1, 2)m_c m_s^2 - 2\hat{I}_1^{[1,0]}(3, 2, 2)m_c m_s^2 + 12\hat{I}_1(1, 1, 4)m_c m_s^2 - 2\hat{I}_2^{[1,0]}(3, 2, 2)m_c m_s^2 + 12\hat{I}_2(1, 1, 4)m_c m_s^2 - 2\hat{I}_0^{[1,0]}(3, 2, 2)m_c m_s^2 + 6\hat{I}_2(3, 1, 2)m_c m_s^2 + 12\hat{I}_0(1, 1, 4)m_c m_s^2 - 4\hat{I}_2(3, 1, 2)m_s^3$$

$$\begin{aligned}
 &+2\hat{I}_2^{[1,0]}(3, 2, 2)m_s^3 - 12\hat{I}_2(1, 1, 4)m_s^3 \\
 &-4\hat{I}_2(2, 1, 3)m_s^3 - 2\hat{I}_2(2, 2, 2)m_s^3 \\
 &+2\hat{I}_2(3, 1, 1)m_c - 4\hat{I}_2^{[1,0]}(3, 2, 1)m_c \\
 &-4\hat{I}_1^{[0,1]}(3, 1, 2)m_c + 4\hat{I}_0(1, 2, 2)m_c \\
 &-2\hat{I}_1^{[1,0]}(3, 1, 2)m_c + 4\hat{I}_2(1, 2, 2)m_c \\
 &+8\hat{I}_0(2, 1, 2)m_c + 8\hat{I}_2(2, 1, 2)m_c \\
 &+2\hat{I}_0(3, 1, 1)m_c + 4\hat{I}_1(1, 2, 2)m_c \\
 &-6\hat{I}_1^{[1,0]}(3, 2, 1)m_c + 2\hat{I}_0(2, 2, 1)m_c \\
 &-4\hat{I}_0^{[0,1]}(3, 1, 2)m_c - 4\hat{I}_2^{[0,1]}(3, 1, 2)m_c \\
 &+2\hat{I}_2^{[1,1]}(3, 2, 2)m_c + 2\hat{I}_1^{[1,1]}(3, 2, 2)m_c \\
 &+2\hat{I}_1(2, 2, 1)m_c + 6\hat{I}_1(2, 1, 2)m_c \\
 &+2\hat{I}_0^{[1,1]}(3, 2, 2)m_c - 6\hat{I}_0^{[1,0]}(3, 2, 1)m_c \\
 &-2\hat{I}_1(3, 1, 1)m_c + 8\hat{I}_1^{[1,0]}(2, 1, 3)m_s \\
 &+4\hat{I}_2^{[1,0]}(3, 2, 1)m_s + 12\hat{I}_1(1, 1, 3)m_s \\
 &-4\hat{I}_2(1, 2, 2)m_s + 2\hat{I}_2^{[0,1]}(2, 2, 2)m_s \\
 &-2\hat{I}_2(2, 2, 1)m_s + 4\hat{I}_2^{[0,1]}(3, 1, 2)m_s \\
 &-2\hat{I}_2^{[1,1]}(3, 2, 2)m_s + 4\hat{I}_1(2, 1, 2)m_s \\
 &+4\hat{I}_2(1, 1, 3)m_s + 4\hat{I}_0(2, 1, 2)m_s \\
 &-10\hat{I}_2(2, 1, 2)m_s + 2\hat{I}_2^{[1,0]}(2, 2, 2)m_s \\
 &+4\hat{I}_2^{[0,1]}(2, 1, 3)m_s + 20\hat{I}_0(1, 1, 3)m_s,
 \end{aligned}$$

where

$$\begin{aligned}
 \hat{I}_\mu^{[\alpha,\beta]}(a, b, c) &= [M_1^2]^\alpha [M_2^2]^\beta \frac{d^\alpha}{d(M_1^2)^\alpha} \frac{d^\beta}{d(M_2^2)^\beta} \\
 &\times [M_1^2]^\alpha [M_2^2]^\beta \hat{I}_\mu(a, b, c), \\
 \hat{I}_k(a, b, c) &= i \frac{(-1)^{a+b+c+1}}{16\pi^2 \Gamma(a)\Gamma(b)\Gamma(c)} (M_1^2)^{1-a-b+k} \\
 &\times (M_2^2)^{4-a-c-k} U_0(a+b \\
 &+c-5, 1-c-b), \\
 \hat{I}_m(a, b, c) &= i \frac{(-1)^{a+b+c+1}}{16\pi^2 \Gamma(a)\Gamma(b)\Gamma(c)} (M_1^2)^{-a-b-1+m} \\
 &\times (M_2^2)^{7-a-c-m} U_0(a+b \\
 &+c-5, 1-c-b), \\
 \hat{I}_6(a, b, c) &= i \frac{(-1)^{a+b+c+1}}{32\pi^2 \Gamma(a)\Gamma(b)\Gamma(c)} (M_1^2)^{3-a-b} \\
 &\times (M_2^2)^{3-a-c} U_0(a+b \\
 &+c-6, 2-c-b), \\
 \hat{I}_n(a, b, c) &= i \frac{(-1)^{a+b+c}}{32\pi^2 \Gamma(a)\Gamma(b)\Gamma(c)} (M_1^2)^{-4-a-b+n} \\
 &\times (M_2^2)^{11-a-c-n} U_0(a+b \\
 &+c-7, 2-c-b),
 \end{aligned}$$

where  $k = 1, 2, m = 3, 4, 5$  and  $n = 7, 8$ . We can define the function  $U_0(a, b)$  as:

$$\begin{aligned}
 U_0(a, b) &= \int_0^\infty dy (y + M_1^2 + M_2^2)^a y^b \\
 &\times \exp \left[ -\frac{B_{-1}}{y} - B_0 - B_1 y \right],
 \end{aligned}$$

where

$$\begin{aligned}
 B_{-1} &= \frac{1}{M_2^2 M_1^2} (m_s^2 (M_1^2 + M_2^2)^2 - M_2^2 M_1^2 Q^2), \\
 B_0 &= \frac{1}{M_1^2 M_2^2} (m_s^2 + m_c^2) (M_1^2 + M_2^2), \\
 B_1 &= \frac{m_c^2}{M_1^2 M_2^2}.
 \end{aligned}$$

### References

1. R. Casalbuoni, A. Deandrea, N. Di Bartolomeo, R. Gatto, F. Feruglio, G. Nardulli, Phys. Rept. **281**, 145 (1997)
2. M.E. Bracco, M. Chiapparini, F.S. Navarra, M. Nielsen, Phys. Lett. B **659**, 559 (2008)
3. F.S. Navarra, M. Nielsen, M.E. Bracco, M. Chiapparini, C.L. Schat, Phys. Lett. B **489**, 319 (2000)
4. F.S. Navarra, M. Nielsen, M.E. Bracco, Phys. Rev. D **65**, 037502 (2002)
5. M.E. Bracco, M. Chiapparini, A. Lozea, F.S. Navarra, M. Nielsen, Phys. Lett. B **521**, 1 (2001)
6. B.O. Rodrigues, M.E. Bracco, M. Nielsen, F.S. Navarra, Nucl. Phys. A **852**, 127 (2011)
7. R.D. Matheus, F.S. Navarra, M. Nielsen, R.R. da Silva, Phys. Lett. B **541**, 265 (2002)
8. R.R. da Silva, R.D. Matheus, F.S. Navarra, M. Nielsen, Braz. J. Phys. **34**, 236 (2004)
9. Z.G. Wang, S.L. Wan, Phys. Rev. D **74**, 014017 (2006)
10. Z.G. Wang, Nucl. Phys. A **796**, 61 (2007)
11. F. Carvalho, F.O. Duraes, F.S. Navarra, M. Nielsen, Phys. Rev. C **72**, 024902 (2005)
12. M.E. Bracco, A.J. Cerqueira, M. Chiapparini, A. Lozea, M. Nielsen, Phys. Lett. B **641**, 286 (2006)
13. L.B. Holanda, R.S. Marques de Carvalho, A. Mihara, Phys. Lett. B **644**, 232 (2007)
14. R. Khosravi, M. Janbazi, Phys. Rev. D **87**, 016003 (2013)
15. R. Khosravi, M. Janbazi, Phys. Rev. D **89**, 016001 (2014)
16. M. Janbazi, N. Ghahramany, E. Pourjafarabadi, Eur. Phys. J. C **74**, 2718 (2014)
17. M.E. Bracco, M. Chiapparini, F.S. Navarra, M. Nielsen, Prog. Part. Nucl. Phys. **67**, 1019 (2011). [arXiv:1104.2864](https://arxiv.org/abs/1104.2864) [hep-ph]
18. P. Colangelo, A. Khodjamirian. [arXiv:hep-ph/0010175](https://arxiv.org/abs/hep-ph/0010175)
19. V.V. Kiselev, A.K. Likhoded, A.I. Onishchenko, Nucl. Phys. B **569**, 473 (2000)
20. R. Khosravi1, M. Janbazi, Phys. Rev. D **87**, 016003 (2013)
21. M.A. Shifman, A.I. Vainshtein, V.I. Zakharov, Nucl. Phys. B **147**, 385 (1979)
22. B.L. Ioffe, Prog. Part. Nucl. Phys. **56**, 232 (2006)
23. J. Beringer et al., Particle Data Group. Phys. Rev. D **86**, 010001 (2012)
24. M. Artuso et al., CLEO Collaboration. Phys. Rev. Lett. **99**, 071802 (2007)
25. G.L. Wang, Phys. Lett. B **633**, 492 (2006)

26. Z.G. Wang, Eur. Phys. J. C **52**, 553 (2007)
27. C. Isola, M. Ladisa, G. Nardulli, P. Santorelli, Phys. Rev. D **68**, 114001 (2003)
28. C. Isola, M. Ladisa, G. Nardulli, T.N. Pham, P. Santorelli, Phys. Rev. D **64**, 014029 (2001)
29. R. Fleischer, Z. Phys. C **58**, 483 (1993)
30. R. Fleischer, Z. Phys. C **62**, 81 (1994)
31. M. Ciuchini, E. Franco, G. Martinelli, L. Reina, L. Silvestrini, Phys. Lett. B **316**, 127 (1993)
32. M. Ciuchini, E. Franco, G. Martinelli, L. Reina, Nucl. Phys. B **415**, 403 (1994)
33. A. J. Buras, [arXiv:hep-ph/9806471](https://arxiv.org/abs/hep-ph/9806471)
34. M. Bando, T. Kugo, K. Yamawaki, Phys. Rept. **164**, 217 (1988)
35. S. Ahmed et al., CLEO Collaboration. Phys. Rev. Lett. **87**, 251501 (2001)
36. C.P. Jessop et al., CLEO Collaboration. Phys. Rev. Lett. **85**, 2881 (2000)
37. E. Eckhart et al., CLEO Collaboration. Phys. Rev. Lett. **89**, 251801 (2002)